

NiO-CGO Composite for SOFC Anode: Synthesis and Characterization

Beatriz Cela¹, Daniel Araújo de Macedo¹, Graziele Lopes de Souza², Auristela Carla de Miranda¹, Antonio Eduardo Martinelli¹, Rubens Maribondo do Nascimento¹ and Carlos Alberto Paskocimas¹

1. PPGCEM, CCET, Federal University of Rio Grande do Norte, 1524 – 59072-970 Natal, RN, Brazil

2. Chemical Engineering Department, CT, Federal University of Rio Grande do Norte, Natal 1524 – 59072-970, RN, Brazil

Received: December 11, 2009 / Accepted: January 05, 2010 / Published: May 25, 2010.

Abstract: In this work compounds of gadolinium-doped ceria, $\text{Ce}_{0.9}\text{Gd}_{0.1}\text{O}_{1.95}$ (CGO) and NiO were synthesized by polymeric precursor method. $\text{NiO-Ce}_{0.9}\text{Gd}_{0.1}\text{O}_{1.95}$ composite was attained by mixture of the powders of the both phases calcinated already. The precursor powders were characterized by simultaneous thermogravimetry-differential thermal analysis and the calcined materials were studied by X-ray diffraction, scanning electronic microscopy, Fourier transform infrared spectroscopy and dilatometry. The refinement of the diffraction data indicated that the powders were crystallized in the wanted phases. All the produced powders had nanometric and sub micrometric features. The produced composite showed good characteristics for the use as anode for SOFC.

Key words: Solid oxide fuel cell, anode, gadolinium-doped ceria, composite, synthesis.

1. Introduction

The direct utilization of hydrocarbons such as natural gas, propane and other liquid fuels without pre-reforming makes the Solid Oxide Fuel Cell (SOFC) potentially more competitive with the current energy conversions technologies. It can significantly reduce the system cost and is therefore highly desirable. The Intermediate Temperature SOFC offer several advantages over the High Temperature SOFC, which includes better thermal compatibility among components, fast start with lower energy consumption, manufacture and operation cost reduction [1].

The CeO_2 based materials are alternatives to the Yttria Stabilized Zirconia (YSZ) to application in SOFC, as they have higher ionic conductivity and less ohmic losses comparing to YSZ. CeO_2 -based SOFCs are largely limited to low temperature applications

where the electronic conduction in CeO_2 electrolytes and the propensity for dimensional change due to loss of oxygen in reducing atmospheres can be significantly suppressed [2]. These electrolytes based in ceria require special electrodes with a higher performance and chemical and thermo mechanical compatibility [3].

A cermet anode appears to be a good choice to find all the requirements demanded by the SOFC, including compatibility with the based-ceria electrolytes. The main preoccupation when a cermet anode is the topic, is the possible chemical reaction between the ceramic and the metallic phase. Without the chemical stability the shrinkage of triple phase boundary would happens, decreasing the active reaction sites and efficiency of the cell [4].

The introduction of Ni in a doped ceria matrix can be a good way to achieve enough electronic conductivity to avoid electric loses, besides act as a catalytic material to the methane crack reaction [5]. The conventional Ni-based anode is prone to promoting carbon formation in handling steam-free hydrocarbons

Corresponding author: Beatriz Cela (1986-), female, PhD student, research field: development of ceramic materials for solid oxide fuel cells. Present address: Zentralabteilung Technologie (ZAT), Forschungszentrum Jülich GmbH, 52425 Jülich, Germany. E-mail: b.cela@fz-juelich.de

although catalyst for the fuel oxidation reaction [3]. Although another noticeable advantage for CeO₂-based anodes is the exceptional tolerance to higher sulfur levels in the fuel stream [5]. This is probably the result of a stronger chemical affinity between CeO₂ and S than between Ni and S. Under typical SOFC operating conditions, Ce₂O₂S is thermodynamically stable and constantly keeps S away from Ni, leaving Ni uncovered by S [2].

The important functions of the gadolinium doped cerium oxide particles Ce_{x-1}Gd_xO_{2-x/2} (CGO) in this ceramic-metal composite (cermet) Ni-CGO should be: supply the Triple Phase Boundary (TPB) with oxide ions, avoid the Ni particles sinterization, and CGO in cermet serves as a supporting framework for Ni particles, thus, ensuring anode thermal expansion acceptably close to other SOFC components [5]. For its properties, the cermet can be used as a high performance electrode.

Furthermore, both the Ni and CGO phase should form continuous network structure respectively in order to extend the effective Ni-CGO-fuel triple-phase boundary deep into the anode layer [6].

Composite anode has been synthesized by several methods, like co-precipitation, polymeric precursors, combustion, solid state reaction [7-10]. This composite can be attained by polymeric precursors method, even from the resin mixture, because the Ni do not form solid solution with the cerium or gadolinium oxides, although the literature do not have a consensus about the Ni solubility in CeO₂ [9].

Several researches showed the importance of the anode layer microstructure development, including initial anode material particle properties, such as particle size distribution, the degree of agglomeration, and metal to ceramic phase ratio [11-14]. The main problem in developing the anode layer comes from the extended Ni particle-coarsening during thermal treatment and subsequent cell operation [6, 15, 16]. Although the loss of the percolation between metallic grains with time and thus the decrease of the

triple-phase boundary length can not be avoided completely, it can be reduced substantially by choosing a preparation path which yields well-mixed nanosized particles after the synthesis [6].

In this study was developed an alternative synthesis methodology in order to obtain cermets with an adequate contact area between electrocatalyst (Ni) and ionic conductor (CGO). The Ni-CGO (NiO-Ce_{0.9}Gd_{0.1}O_{1.95}) cermet was obtained by “two steps synthesis”, which consisted of mixture of NiO and CGO phases pre synthesized by the polymeric precursor method. To reach approximately 39% of metallic phase in the final anode layer was determined that 50% of NiO phase was need in the composite [17]. The materials were characterized by X-ray diffraction (XRD), scanning electronic microscopy (SEM), Fourier transform infrared spectroscopy (FTIR), simultaneous thermogravimetry-differential thermal analysis (TG/DTA) and dilatometry. The advantages of the method and the characteristics of the materials produced have been investigated.

2. Synthesis and Characterization Methods

The production of this composite had two steps. At first step was to produce nanopowders of both phases separately. CGO and NiO were synthesized by the polymeric precursor method in two syntheses. The synthesis by the polymeric precursor method were performed with the same proportion of citric acid : metallic cations, 3.5 : 1, and also the same ratio of citric acid : ethylene glycol mass, respectively 60 : 40. The starting materials used were cerium nitrate hexahydrate (VETEC, Brazil) 99.0%, gadolinium nitrate hexahydrate (Sigma Aldrich, Germany) 99.9% and nickel nitrate hexahydrate (VETEC, Brazil) 98.0%.

The precursor resins of CGO and NiO were expanded at 300 °C and 350 °C, respectively, and dwell time 1 h. Following process was calcination, that was previous determined by experiments, equal for both powders, 800 °C for 2 h.

As a second step both phases' powders were mixed

in a 50-50 weight % proportion, by milling under 60 rpm rotation during 2 h. The composite powder was used to prepare sample pellets by compaction. The pellets were sinterized in air at 1300 °C for 30 min. Samples of the anode were also submitted to thermal treatment in H₂ pure atmosphere, 900 °C during 1 h, to reduce the NiO and be able to analysis this effect.

The characterization of the composite material was performed by several methods in different parts of the experiments. Expanded resin powders' preliminary analyses were made using a TG/DTA simultaneous analyzer model STA 409C Netzsch, from 25 °C to 1000 °C and synthetic air atmosphere. The XRD analyses were made in Shimadzu/XRD-6000 equipment, using CuK_α radiation, with 40 kV and 40 mA. The present phases and crystallite average size (D_{DRX}) were calculated through Rietveld XRD data refinement with the program BDWS-9807 [18]. The FWHM corrections were made with the lanthanum-hexaborate (LaB₆). After the corrections it is possible to calculate the crystallite average size and micro deformation. The crystallite size D_{DRX} is calculated according Scherrer equation (Eq. (1)), and the micro deformation ε is calculated by the Williamson-Hall method (Eq. (2)), where λ is the material's radiation wave-length using the diffractometer, θ is the corresponding Bragg angle, B is the FWHM of a diffraction peak, D_{DRX} is the crystallite size and ε is the net micro deformation.

$$D_{XRD} = (0.9\lambda)/(B\cos\theta) \quad (1)$$

$$B\cos\theta = (0.9\lambda/D_{XRD}) + (2\varepsilon)\sin\theta \quad (2)$$

The synthesized powders samples' morphologies were analyzed by SEM, as well as the sintered composite microstructures. The sintered pellets were polished and thermally attacked to reveal the grain boundaries. The average grain size could be determined by intercept method.

An infrared spectrum of the NiO-CGO composite was recorded with FTIR (IR Prestige-21, Schimadzu) in the 400-4600 cm⁻¹ spectral range. A dilatometer (BP Engenharia RB-115, Brazil) was used to study the shrinkage behaviour at a constant heating rate (CHR)

of 3 °C/min up to 1300 °C (without holding) and to determine the coefficient of thermal expansion (CTE) of the sintered composite at 1300 °C for 0.5 h. The CTE was measured in air in the temperature range from 200 to 1000 °C.

3. Results and Discussion

3.1 Thermal Analyses

The TG and DTA analyses (Fig. 1) were made on the as prepared powders after the resin expansion, first thermal treatment, which was at 300 °C for the CGO precursor and 350 °C for the NiO precursor. The temperature in which the CGO precursor started to mass loss was exactly at 300 °C and the NiO precursor at 350 °C, conform expected. The big mass loss was due to the carbon present in both expanded resins, originating from the degradation of the polymer formed by the reaction of polyesterification (metallic citrate and ethylene glycol). The mass loss

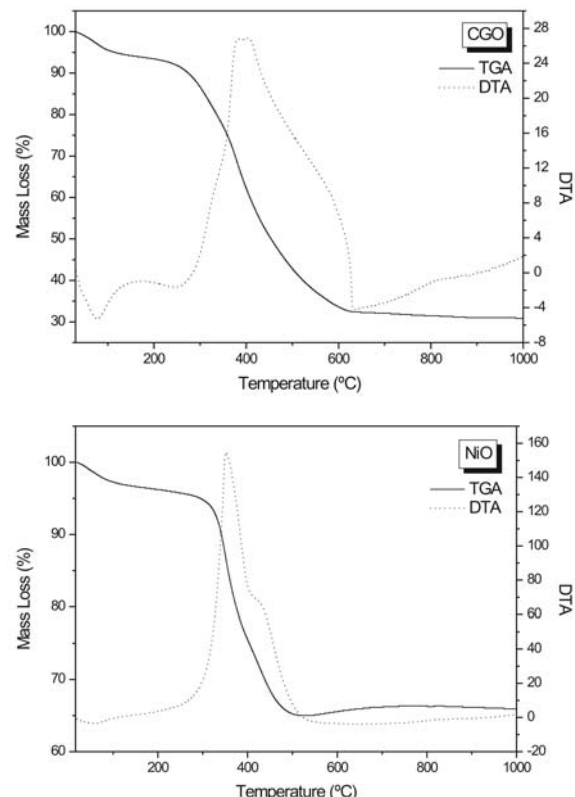


Fig. 1 TGA and DTA analyses of the precursors of CGO and NiO powders.

stabilizes around 600 °C for the CGO and 500 °C for the NiO. According to the DTA data the reactions stabilization occurs 50 °C above the mass loss stabilization in both cases. These results indicate that starting on 650 and 600 °C crystalline CGO and NiO, respectively, can be obtained. Besides this the temperature of 800 °C was the chosen one for calcination of both phases due to previous XRD data showing better crystallized phases at this temperature.

3.2 Structure

Fig. 2 displays the XRD pattern of the NiO-CGO composite obtained after calcination of both phases at 800 °C for 2 h. XRD data revealed no peaks of secondary phases, i.e., there is no obvious peaks from phases other than NiO (JCPDS 47-1049) and CGO (JCPDS 75-0161) until the detection limit of the XRD. The Rietveld refinement data are illustrated in Table 1, the data were obtained using the program BDWS-9807. NiO and CGO powders exhibit cubic structures with space group Fm-3m and crystallite size (D_{XRD}) in the range of 45-48 nm. The refinement quality can be checked by the S value, which is obtained by the expression $S = R_{wp}/R_{exp}$. The low S value got in this work indicates that the data were successfully refined.

3.3 FTIR Spectroscopic Analysis

The FTIR spectrum of NiO-CGO composite (Fig. 3) shows that the absorption bands in low wave number region are associated to the oxygen-metal link. The enlarged bands in $\sim 3500 \text{ cm}^{-1}$ are attributed to the stretching vibration of the hydrogen-bonded OH groups present. The bands referents to water in the material (3420 cm^{-1}) were present on the sample. After the thermal treatment at 800 °C for 2 h, the carbon bands were nearly eliminated. Indicating a residual carbon some bands still can be find in the calcinated samples, for example associated to carboxylate anion (COO^-) stretching and the C=O groups or to stretching vibration of the C-O bonds (1620 cm^{-1} , 1389 cm^{-1} and 1060 cm^{-1}).

3.4 Sintering Behaviour and Thermal Expansion Coefficient (CET)

The dilatometry technique first was used to verify the sintering behaviour of the composite, as this is a very important part of the composite processing. The result shows that the sintering process occurs around 1200, lower than previously reported in literature for the same composition and ratio of NiO and CGO [4]. As was desirable certain porosity on the pressed sample the sintering conditions chosen were 1300 °C only for 30 min, also avoiding grain growth.

Fig. 5 displays the thermal expansion plot for the NiO-CGO composite sintered at 1300 °C for 0.5 h. We used linear fittings to deal with the experimental data. The thermal expansion coefficient (CTE) was found to

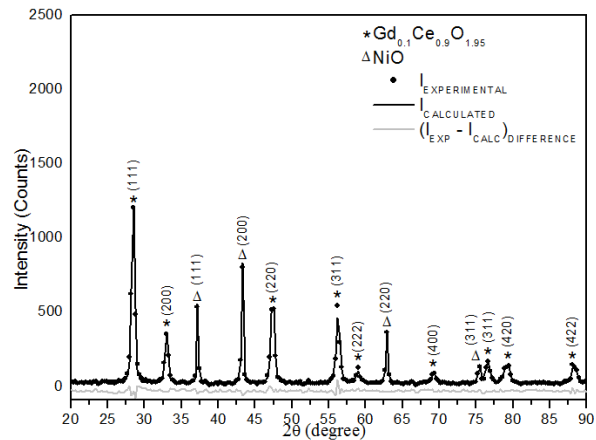


Fig. 2 XRD pattern of the NiO-CGO composite.

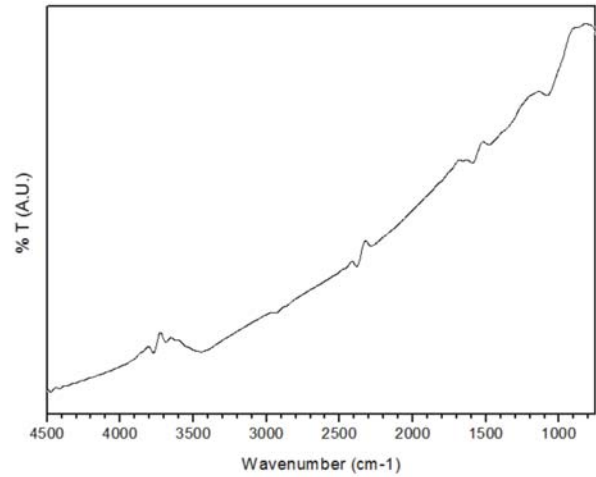


Fig. 3 FTIR spectrum of the CGO-NiO composite.

Table 1 Crystallographic data attained by Rietveld refinement of XRD results.

	a=b=c (Å)	d (Å)	D _{XRD} (nm)	ε (%)	Weight %	U	V	W
Ce _{0.9} Gd _{0.1} O _{1.95}	5.4180	1.7624	45.84	0.0695	48.56	0.000000	0.090181	0.003594
NiO	4.1760	1.6877	47.82	0.0782	51.44	0.000000	0.044023	0.022630

be $13.26 \times 10^{-6} \text{ }^{\circ}\text{C}^{-1}$, this value is in agreement with that reported by Gil et al. [17], which is very close to that of gadolinium-doped ceria and which is the choice of electrolyte for intermediate temperature solid oxide fuel cell. The coefficient of thermal expansion of the anode material should match that of the other cell components to prevent cracking during the thermal cycles.

3.5 Morphologie

The Fig. 6 shows SEM pictures of CGO (Fig. 6a) and NiO (Fig. 6b) powders obtained by the polymeric precursor method and calcined at 800 °C for 2 h in air. The powders exhibit strong presence of agglomerates of nanoparticles (some smaller than 100 nm). This particle size is essential to obtain the NiO-CGO nanocomposite. The agglomerates, probably formed during the calcination, were not dispersed by ultrasonic agitation prior to SEM analysis. So the aforesaid crystallites (< 48 nm) of the powders indicate that the fundamental size of their particles is of nanometer scale only and nanosize particles can be formed from it if the powders could be efficiently de-agglomerated.

Figs. 7 and 8 show the microstructures of the fracture surfaces of the NiO-CGO composite sintered and of the Ni-CGO cermet obtained after thermal treatment in H₂ atmosphere. The morphologies of sintered and reduced samples are a bit different. It can be seen that the reduced sample has a higher concentration of pores in the CGO matrix. It is also possible to observe that the phase dispersion did not happen in a nanometric scale, producing small agglomerate of phases. Gil et al. [17] have been prepared anode microstructures with high interconnected porosity (25% total porosity) and good connections between particles, especially between Ni-Ni grains (maintaining the continuity in the metallic phase) which are essential to improve the

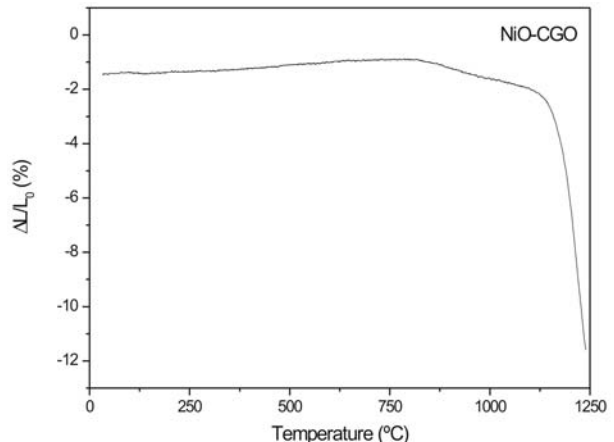


Fig. 4 Dilatometry analysis of the composite sintering behaviour.

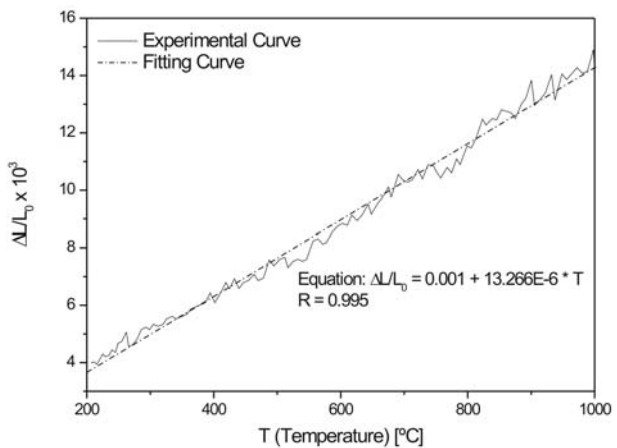
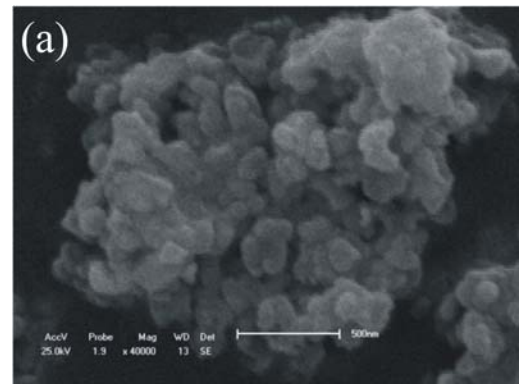


Fig. 5 Thermal expansion plot of the NiO-CGO sintered at 1300 °C for 0.5 h.



(to be continued)

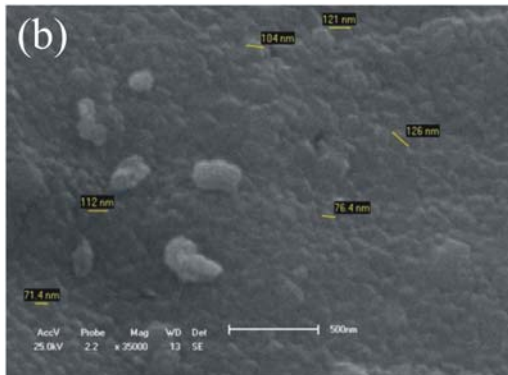


Fig. 6 SEM pictures of the CGO (a) and NiO (b) powders.

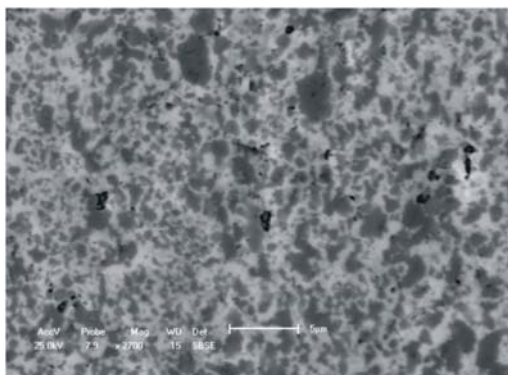


Fig. 7 SEM picture of the sintered NiO-CGO pellet.

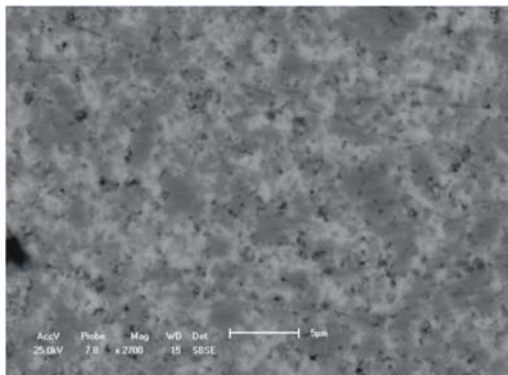


Fig. 8 SEM picture of Ni-CGO pellet reduced in H_2 atmosphere.

triple phase boundary (TPB) area where reaction between hydrogen, Ni and CGO takes place. As in this study were not used pore forming materials, the total porosity (calculated by image processing) was less than 10%. In future studies we will study the addition of citric acid as pore-forming.

4. Conclusions

The polymeric precursor method using citric acid,

nitrates and ethylene glycol is a simple and efficient method to obtain homogeneous nanoparticles and without non desirable phases. The results showed that the two steps synthesis method was successful to produce the NiO-CGO composite and that the composite precursor's particles (pre calcinated) are essential to the achievement of a good sub micrometric composite. In the sintered composite the Ni percolating phase can be good in the electronic conductivity, which together with the morphologic characteristics of the powders indicates that the material processed in this way is a good candidate to SOFC anode material. CTE value obtained for composite is very close to that of gadolinium-doped ceria electrolytes. Other experiments need to be performed, such as the use of pore forming materials to increase the anode porosity and electrochemical analyses to check electronic and ionic conductivity.

References

- [1] B.C.H. Steele, Appraisal of $Ce_{1-y}Gd_yO_{2-y/2}$ electrolytes for IT-SOFC operation at 500 °C, Solid State Ionics 129 (2000) 95-110.
- [2] K. Huang, J.B. Goodenough, Solid Oxide Fuel Cell Technology: Principles, Performance and Operations, CRC Press, USA, 2009.
- [3] A. Atkinson, et al., Advanced anodes for high temperature fuel cells, Nature Materials 3 (2004) 17-27.
- [4] P. Datta, P. Majewski, F. Aldinger, Synthesis and reactivity study of gadolinia doped ceria-nickel: A potential anode material for solid oxide fuel cell, Journal of Alloys and Compounds 455 (2008) 454-460.
- [5] V. Gil, A. Larrea, R.I. Merino, V.M. Orera, Redox behavior of Gd-doped ceria-nickel oxide composites, Journal of Power Sources 192 (2009) 180-184.
- [6] M. Marinšek, K. Zupan, J. Maèek, Ni-YSZ cermet anodes prepared by citrate/nitrate combustion synthesis, Journal of Power Sources 106 (2002) 178-188.
- [7] S. Zha, W. Rauch, M. Liu, Ni- $Ce_{0.9}Gd_{0.1}O_{1.95}$ anode for GDC electrolyte-based low-temperature SOFCs, Solid State Ionics 166 (2004) 241-250.
- [8] T. Ishihara, T. Shibayama, H. Nishiguchi, Y. Takita, Nickel-Gd-doped CeO_2 cermet anode for intermediate temperature operating solid oxide fuel cells using $LaGaO_3$ -based perovskite electrolyte, Solid State Ionics 132 (2000) 209-216.

- [9] V. Gil, C. Moure, J. Tartaj, Sinterability, microstructures and electrical properties of Ni/Gd-doped ceria cermets used as anode materials for SOFCs, *Journal of the European Ceramic Society* 27 (2007) 4205-4209.
- [10] C. Ding, H. Lin, K. Sato, T. Hashida, Synthesis of $\text{NiO-Ce}_{0.9}\text{Gd}_{0.1}\text{O}_{1.95}$ nanocomposite powders for low-temperature solid oxide fuel cell anodes by co-precipitation, *Scripta Materialia* 60 (2009) 254-256.
- [11] C.H. Lee, C.H. Lee, H.Y. Lee, S.M. Oh, Microstructure and anodic properties of Ni/YSZ cermets in solid oxide fuel cells, *Solid State Ionics* 98 (1997) 39-48.
- [12] S. Primdahl, M. Mogensen, Oxidation of hydrogen on Ni/yttria stabilized zirconia cermet anodes, *Journal of Electrochemistry Society* 144 (1997) 3409-3419.
- [13] J. Abel, A.A. Kornyshev, W. Lehnert, Correlated resistor network study of porous solid oxide fuel cell anodes, *Journal of Electrochemistry Society* 144 (1997) 4253.
- [14] T. Kawada, N. Sakai, H. Yokokawa, M. Dokiya, M. Mori, T. Iwata, Characteristics of slurry-coated nickel zirconia cermet anodes for solid oxide fuel cells. *Journal of Electrochemistry Society* 137 (1990) 3042-3047.
- [15] H. Yokokawa, H. Tu, B. Iwanschitz, A. Mai, Fundamental mechanisms limiting solid oxide fuel cell durability, *Journal of Power Source* 182 (2008) 400-412.
- [16] A.A. Kulikovsky, H. Scharmann, K. Wippermann, Dynamics of fuel cell performance degradation, *Electrochemistry Communications* 6 (2004) 75-82.
- [17] V. Gil, J. Tartaj, C. Moure, Chemical and thermomechanical compatibility between Ni-GDC anode and electrolytes based on ceria, *Ceramics International* 35 (2009) 839-846.
- [18] R.A. Young, A.C. Larson, C.O. Paiva-Santos, Program DBWS-9807A-Rietveld analysis of X-ray and neutrons powder diffraction patterns, User's Guide, 2000.